NACA

RESEARCH MEMORANDUM

SUPERSONIC TUNNEL INVESTIGATION BY MEANS OF INCLINED-PLATE

TECHNIQUE TO DETERMINE PERFORMANCE OF SEVERAL NOSE

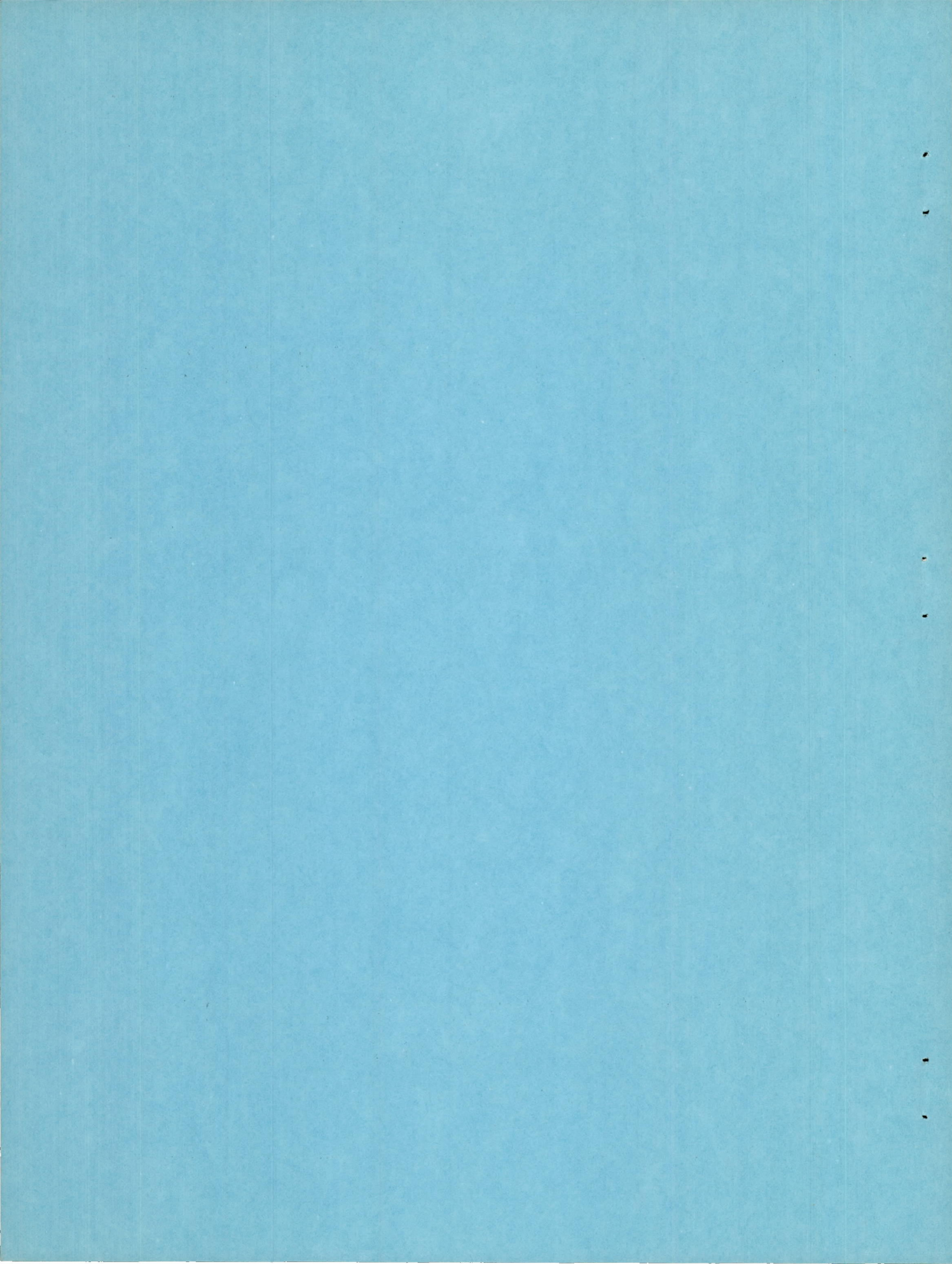INLETS OVER MACH NUMBER RANGE OF 1.72 TO 2.18

By Jerome L. Fox

Lewis Flight Propulsion Laboratory
Cleveland, Ohio

NATIONAL ADVISORY COMMITTEE
FOR AERONAUTICS

WASHINGTON

February 14, 1951

2049

NATIONAL ADVISORY COMMITTEE FOR AERONAUTICS

RESEARCH MEMORANDUM

SUPERSONIC TUNNEL INVESTIGATION BY MEANS OF INCLINED-PLATE

TECHNIQUE TO DETERMINE PERFORMANCE OF SEVERAL NOSE

INLETS OVER MACH NUMBER RANGE OF 1.72 TO 2.18

By Jerome L. Fox

SUMMARY

A suspended flat plate was used to continuously vary the Mach number in the NACA Lewis 18- by 18-inch Mach number 1.91 supersonic tunnel. The useful range of the tunnel was extended over a range of Mach numbers from 1.72 to 2.18. Maximum variations in the Mach number of the flow produced at the vicinity of nose inlets at zero angle of attack were ±0.01 and flow angularities were less than approximately 0.35°.

The technique was applied to the determination of pressure recovery and mass-flow characteristics of four supersonic nose inlets over the Mach number range produced.

INTRODUCTION

A technique that permits a variable Mach number investigation to be conducted in existing fixed-Mach-number tunnels has been investigated. The method utilizes the uniform flow after a two-dimensional expansion or compression produced by the leading edge of a flat plate suspended upstream of the diffuser inlet. A form of this technique, used to depress a tunnel Mach number to values near 1 in order to test airfoils in the transonic range, has been reported by the Flygtekniska Forsoksanstalten (Stockholm).

As an application of the technique, the cold performance in terms of pressure recovery and mass flow was determined over the range of Mach numbers produced for four supersonic nose inlets, including (1) a single-shock spike inlet, (2) a curved-spike inlet, (3) a perforated convergent-divergent diffuser, and (4) a single-shock spike inlet with a perforated cowl.

APPARATUS AND PROCEDURE

Apparatus

The investigation was conducted in the NACA Lewis 18- by 18-inch Mach-number-1.91 tunnel. Inlet stagnation temperatures were maintained at approximately 150° F with an inlet total pressure approximately atmospheric. Dew points during running were -10° F or less. Flow patterns in the vicinity of the inlets were observed with a two-mirror schlieren apparatus and recorded photographically.

Three plates, similar in plan form, consisting of one flat plate and two plates bent approximately 5° in opposite directions, were used in the investigation. Principal dimensions of the plates are shown in figure 1. Two bent plates were fabricated in order to yield flow at an angle of attack of approximately 5° to the models. The plate angles are not identical due to an error in machining. All plates were machined from 3/8-inch steel and during operation were bolted to three supports that were silver soldered to the diffusers. A photograph of a complete configuration in position in the tunnel is presented in figure 2. Design dimensions of the plates and supports were determined by the consideration that the plate must be so positioned with respect to the inlet that the inlet is completely downstream of the shock or expansion fan originating at the leading edge of the plate for all operating conditions. In addition, the width of the plates must be such that the disturbance from the tips of the leading edge shall fall downstream of the inlet and of the perforations, if used.

A photograph of the inlets and projecting spikes used in this investigation is shown in figure 3. Sketches including principal dimensions are presented in figure 4. The supersonic diffusers included: (1) a 25° half-angle single-shock spike inlet with a curved cowl, (2) an all-external compression inlet with a curved spike designed to produce nearly isentropic compression, (3) a perforated convergent-divergent inlet with an over-all contraction ratio of 1.531, and (4) a 20° half-angle single-shock spike inlet with a perforated cowl.

A schematic diagram of the subsonic diffusers used in conjunction with the inlets of figure 4 is shown in figure 5(a). Subsonic diffuser 1, used with the projecting spike inlets, was that of reference 1. Diffuser 2, which was used with the perforated convergent-divergent inlet, was the same as that used in the investigation of reference 2. Both diffusers have a maximum total expansion angle of 5° and are faired into a 3.6-inch-diameter simulated combustion chamber 11.75 inches long. Total pressure of the air flowing through the combustion chamber was measured by the 40-tube equal-area pitot-static rake of figure 5(b).

The vertical and horizontal wedge rakes used to calibrate the flow in the vicinity of the inlets are shown in figure 6. The wedges have 15° half angles and are 3/8-inch wide and 1/8-inch thick. They were instrumented with top and bottom static orifices and top and bottom pitot tubes. The pitot tubes were mounted parallel to the wedge surfaces and behind the static orifices to prevent interference.

PROCEDURE

Initial calibration runs were designed to ascertain conditions of the flow in the vicinity of the inlets. The angle made by the plate with the tunnel axis was varied by means of the angle of attack mechanism of the diffuser support body in increments of approximately 1° to a maximum value of ±7°. These runs were made with both the flat plate and the two bent plates. Two bent plates were required because of the physical limitations of the test setup. The use of only one plate to furnish flow at a 5° angle of attack over the entire Mach number range contemplated would have required rotation of the subsonic diffuser 12° in one direction. Angles of this magnitude were not possible because the configuration at this attitude would cause excessive flow blockage and interference between the plate and tunnel walls.

After calibration, runs were made to determine the performance of the four inlets investigated at five free-stream Mach numbers M_0 ranging from 1.72 to 2.18. An additional run with several spike tip projections was made for the curved spike inlet at M_0 of 1.80. Several preliminary runs were also made with the single-shock perforated-cowl inlet using various distributions of perforation area in an attempt to swallow the normal shock at the nominal design Mach number of 1.80.

The mass flows through the unit were calculated from the pressures recorded by the pitot-static rake in the combustion chamber. The results are presented in the form of a relative mass-flow ratio m_3/m_1, which represents the ratio of mass flow through the combustion chamber to the mass flow in a free-stream tube of diameter equal to the inlet diameter.

DISCUSSION OF RESULTS

Results of Plate Calibration

Results of the calibration of flow approximately 8 inches behind the leading edge of the plates are presented in figure 7. Two sets of data points are presented for the flat plates. Circles represent average Mach number determined from three horizontal wedges, and squares are values

determined from three wedges mounted in a vertical plane. The area cali-
brated was approximately the size of the inlet areas to be investigated.

Uniform flow was obtained behind the flat plate over a Mach number
range of 1.72 to 2.18. Maximum deviation in Mach number calculated from
any one wedge differed from the average value by ±0.01, and the maximum
flow angularity was ±0.35°.

Mach numbers of flow produced by the flat plate are approximately
0.02 higher than the theoretical curve for $M_0 = 1.91$ (nominal tunnel-
test-section Mach number). This difference is explained by the fact
that the measured plate angle is not the true angle between the plate and
stream direction due to flow angularity in the tunnel. An examination of
a previous tunnel calibration showed that the flow angularities in the
vicinity of the leading edge of the plate over the range of plate angles
investigated were in the proper direction and of approximately the right
magnitude to cause the effects noted.

The test Mach numbers produced by the bent plates also are shown in
figure 7. For Mach numbers below 1.93 the values are in good agreement
with the flat-plate data; above 1.93 the data points fall above the flat-
plate data. This deviation was accompanied by an increase in flow
angularities to a maximum of approximately 0.75°. No explanation has
been found for these differences, but they could have been caused by an
undetected error in attaching plates to the supports or alining the
wedges.

The agreement of the data with theory is not essential to the test-
ing technique, because so long as the flow angularities and Mach number
variations in the test region are not excessive, a calibration curve
would indicate the proper plate angle for any desired test Mach number.

The Mach number range covered in this investigation was limited by
the required size of the plate for the models investigated, by tunnel
size, or by the allowable amount of flow blockage.

Inlet Performance

Summary curves of the pressure recovery and the mass-flow character-
istics of the inlets investigated over a range of Mach numbers from 1.72
to 2.18 are shown in figure 8. Included are pressure recovery and
relative mass-flow ratio at both the point of peak recovery and the
beginning of supercritical operation (point where mass flow remains
constant as outlet area is increased).

2049

All inlets with projecting spikes attained peak recovery when the
normal shock was located in its most upstream stable position on the
spike. At all mass-flow ratios below that corresponding to peak
recovery, the phenomenon of cold buzz (shock oscillation) was observed.

When the inlets were operating at an angle of attack of approxi-
mately 5° (using the bent plates), pressure recoveries were reduced
less than 2 percent from their values at zero angle of attack, whereas
the relative mass-flow ratio for supercritical operation remained almost
unchanged.

Single-shock spike inlet. - The characteristics of the single-shock
spike inlet are shown in figure 8(a). This inlet is the same as one of
the curved-lip configurations of reference 1. Included with the experi-
mental pressure recovery curves is a plot of the theoretical recovery
including only shock losses across the conical shock and across a normal
shock assumed to occur at an average Mach number at the inlet. The data
points at peak recovery fall from approximately 3 to 8 percent below the
theoretical curve. If some reasonable value of pressure recovery is
assumed for the internal diffusion, good agreement between theory and
experiment is indicated.

The experimental values of relative mass-flow ratios appear to be
low. The conical shock strikes the inlet lip at approximately $M_0 = 2.10$,
and at this point the inlet should be operating at a relative mass-flow
ratio of 1.0. The reduction in mass flow was attributed to the fact that
a detached shock wave occurred ahead of the lip at all Mach numbers
investigated.

A series of schlieren photographs illustrating the progressive
changes in the inlet flow pattern with varying free-stream Mach number
is shown in figure 9. The increasing mass-flow ratios with increasing
Mach numbers correspond to the observed movement of the normal shock
closer to the inlet. At elevated Mach numbers the expansion fan from the
leading edge of the plate can be seen, whereas at depressed Mach numbers
the compression shock produced by the plate is clearly visible. At all
Mach numbers a disturbance can be seen that originates on the plate and
apparently strikes the diffuser inlet. This disturbance originates at
the junction of the raked-in portion and the straight back portion of the
plate trailing edge, and is not in the plane of the inlet. At $M_0 = 2.18$
a faint line is apparent above the plate surface ahead of the inlet. This
line is a side view of the trailing vortex sheet shed by the trailing
edge of the raked-in portion of the flat plate.

Curved-spike inlet. - The curved-spike inlet had an initial conical section of 20° half angle followed by a curved section and is a 1/3-scale model, with slight differences in internal design, of the inlet reported in reference 2. The pressure recovery and the mass-flow characteristics for this inlet are presented in figure 8(b). No theoretical curves are presented because their calculation would require a series of lengthy computations using the method of characteristics. The tailed symbols are data from reference 2. The pressure recoveries agree well, but the relative mass-flow ratios of the larger model are approximately 3 to 5 percent higher. This difference can be explained by the slight dissimilarity in internal goemetry. The trends of the mass-flow data, however, show fair agreement. The low relative mass-flow ratios could be caused by internal choking produced by excessive boundary-layer growth in the presence of a strong adverse pressure gradient on the curved spike.

The performance characteristics of this inlet are sensitive to spike tip projection, as shown in figure 10 by the variation of relative mass-flow ratios and peak pressure recovery with spike tip projection at $M_0 = 1.80$. As the tip projection increased beyond the optimum, the relative mass-flow ratio decreased very sharply with only a slight overall change in pressure recovery. Thus, if the curved-spike inlet is to operate at large mass-flow ratios, the spike tip projection must be maintained near its optimum value.

Data obtained with the large-scale model at equivalent tip projection (tailed symbols) show good agreement, except for the value of relative mass-flow ratio at minimum tip projection. A part of this discrepancy may be due to experimental difficulty in establishing the exact relative mass-flow ratio at the point of peak recovery, because the curve of pressure recovery as a function of mass-flow ratio is very flat in the vicinity of peak pressure recovery at $M_0 = 1.80$.

Perforated convergent-divergent inlet. - The performance at varying free-stream Mach number of a representative convergent-divergent perforated inlet chosen from the extensive series of inlets reported in reference 3 is presented in figure 8(c). The particular inlet chosen is inlet 1.531-f of reference 3. Included with the experimental data are theoretical curves for the pressure recovery and relative mass-flow ratio determined from a stepwise integration method outlined in reference 3.

From an analysis based on reference 3, an abrupt swallowing of the normal shock was theoretically expected to occur at $M_0 = 1.77$; however, the data show a gradual transition with the shock only partly swallowed at $M_0 = 1.80$. With the normal shock swallowed ($M_0 \geq 1.91$) the

experimental values of pressure recovery and mass-flow ratios show fair
agreement with the theoretical curves. The tailed symbols at $M_0 = 1.91$
are check points from the investigation of reference 3 for the same
inlet. All values agree to within ±2 percent of pressure recovery or
relative mass-flow ratio.

Single-shock spike, perforated cowl inlet. - Illustrated in
figure 8(d) are the performance characteristics of an inlet designed to
combine the advantages of external compression produced by a projecting
spike and the advantages of large internal contraction utilizing mass-
flow spillage through cowl perforations to remove the maximum contraction
ratio restriction of unperforated inlets.

The inlet was so designed that the conical shock would strike the
inlet lip for a free-stream Mach number of 1.80. Preliminary runs were
made with several distributions of perforated hole area in an attempt to
swallow the normal shock at a Mach number of 1.80. The results of ref-
erence 3 show that for perforated convergent-divergent inlets the value
of the subsonic hole orifice coefficient Q_a was approximately 0.50.
The results presented herein show that the value of Q_a for the con-
figuration of figure 9(d) was of the order of 0.25. The perforations
were not countersunk as they were in the investigation of reference 3,
which would be expected to account for a considerable portion of the
differences in the value of Q_a. The perforation distribution investi-
gated, for which the ratio of a total hole area to throat area was 0.39,
permitted the swallowing of the normal shock at free-stream Mach numbers
greater than 1.85.

In the range of Mach numbers for which the normal shock was not
swallowed, the pressure recovery of this inlet was higher than that of
the perforated convergent-divergent inlet (fig. 8(c)). This higher
recovery is due to the relatively efficient compression produced by the
projecting spike even when the normal shock is ahead of the cowling.
At Mach numbers near 1.9, however, the convergent-divergent inlet had
higher recovery. With the normal shock swallowed, only approximately
7 percent of the maximum mass flow was spilled through the perforations
(fig. 8(d)). In the transition region between Mach numbers 1.80 and
1.90, the experimental curves have been drawn as dashed lines because
the actual trends of the curves were not determined. A comparison of
the pressure recovery with the recoveries of the single-shock spike
inlet and the curved-spike inlet showed the recovery to be 2 to 3 percent
greater than the former and 3 to 4 percent lower than the latter. This
result seems to indicate either that the normal shock was not located
near the throat, so that the shock Mach number was greater than expected,
or that the flow through the perforations disturbed the main flow enough
to appreciabley lower the internal diffuser recovery.

SUMMARY OF RESULTS

A variable Mach number technique was applied to determine the performance characteristics of four types of supersonic nose inlet at several free-stream Mach numbers. The following results were obtained:

1. The technique investigated produced uniform flow over a Mach number range from 1.72 to 2.18 in a tunnel of nominal design Mach number 1.91. At zero angle of attack, maximum variation of Mach number in the vicinity of the inlet was ± 0.01, and maximum flow angularities were approximately 0.35°. The flow produced at an angle of attack of approximately 5° showed increased flow angularities of the order of 0.75°, although variations in the Mach number remained small.

2. The abrupt swallowing of the normal shock theoretically predicted for the perforated convergent-divergent inlet was not realized experimentally, but was replaced by a gradual entry of the shock into the inlet with increasing Mach number.

3. The mass-flow characteristics of the curved-spike inlet exhibited high sensitivity to the spike tip projection. Increasing the spike tip projection beyond its optimum position caused a sharp reduction in the captured mass-flow ratio of the inlet. The maximum pressure recovery for this inlet varied from 0.96 at Mach number 1.72 to 0.83 at Mach number 2.18.

4. For the perforated inlet with projecting cone, about 7 percent of the mass flow passed through the perforations in the Mach number range from 1.9 to 2.18. The maximum pressure recovery decreased from 0.89 to 0.77 in this range of Mach numbers.

Lewis Flight Propulsion Laboratory,
    National Advisory Committee for Aeronautics,
        Cleveland, Ohio.

REFERENCES

1. Moeckel, W. E., Connors, J. F., and Schroeder, A. H.: Investigation of Shock Diffusers at Mach Number 1.85. I - Projecting Single-Shock Cones. NACA RM E6K27, 1947.

2. Obery, L. J., and Englert, G. W.: Force and Pressure Characteristics for a Series of Nose Inlets at Mach Numbers From 1.59 to 1.99. II - Isentropic-Spike All-External Compression Inlet. NACA RM E50J26a.

3. Hunczak, Henry R., and Kremzier, Emil J.: Characteristics of
       Perforated Diffusers at Free-Stream Mach Number 1.90. NACA RM
       E50B02, 1950.
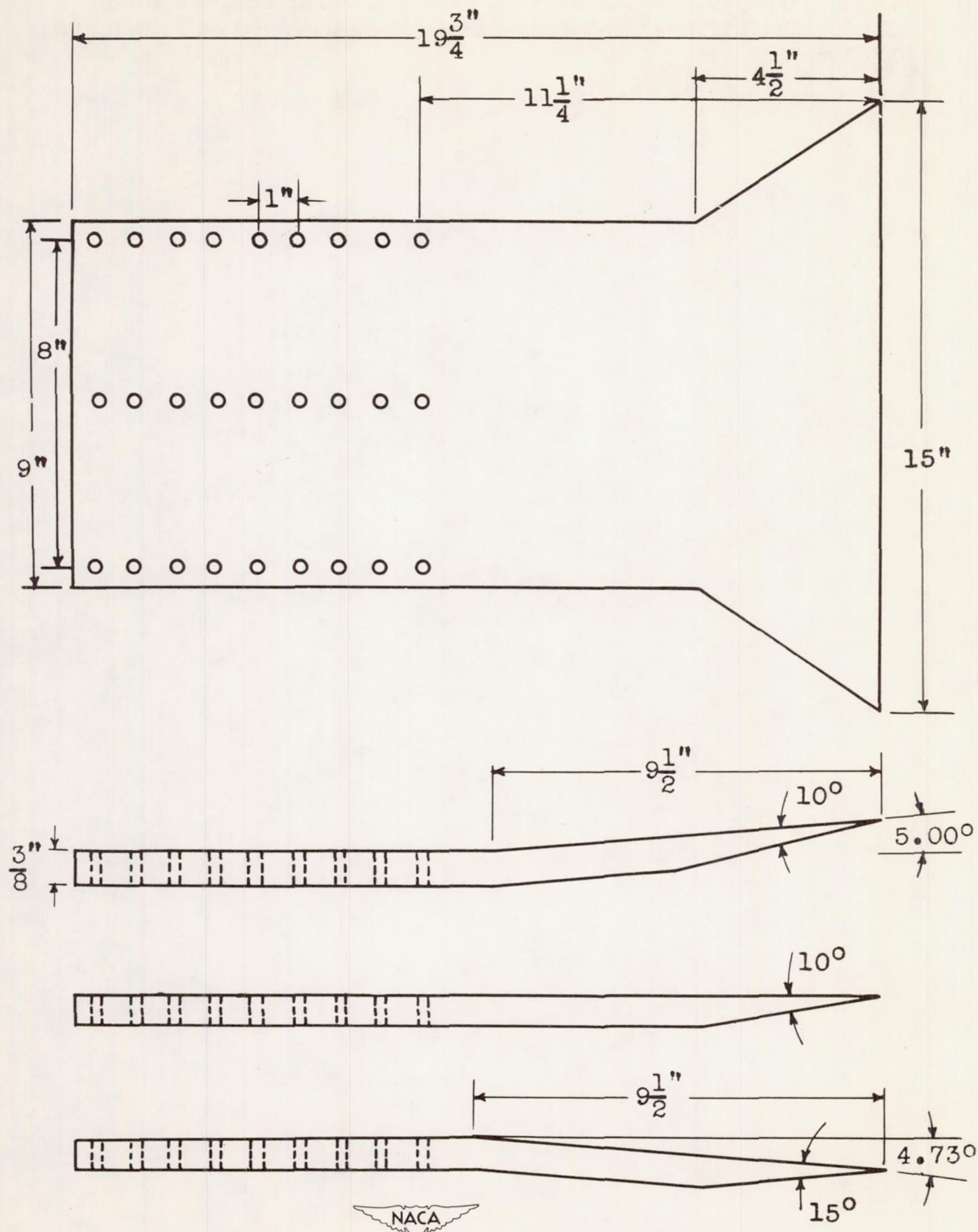
Figure 1. - Flat and bent plates used in investigation.
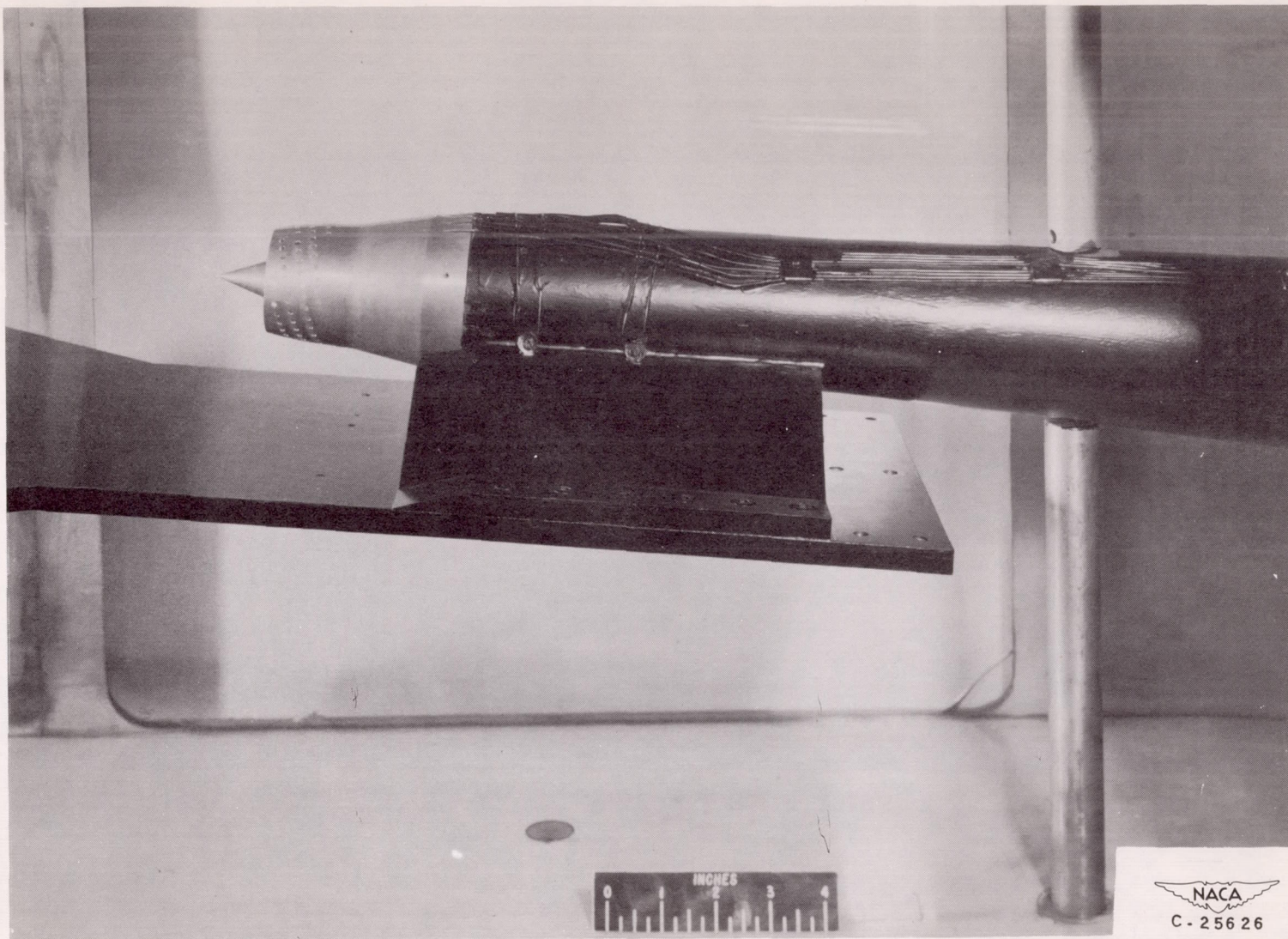
Figure 2. - Complete model configuration in position in tunnel.
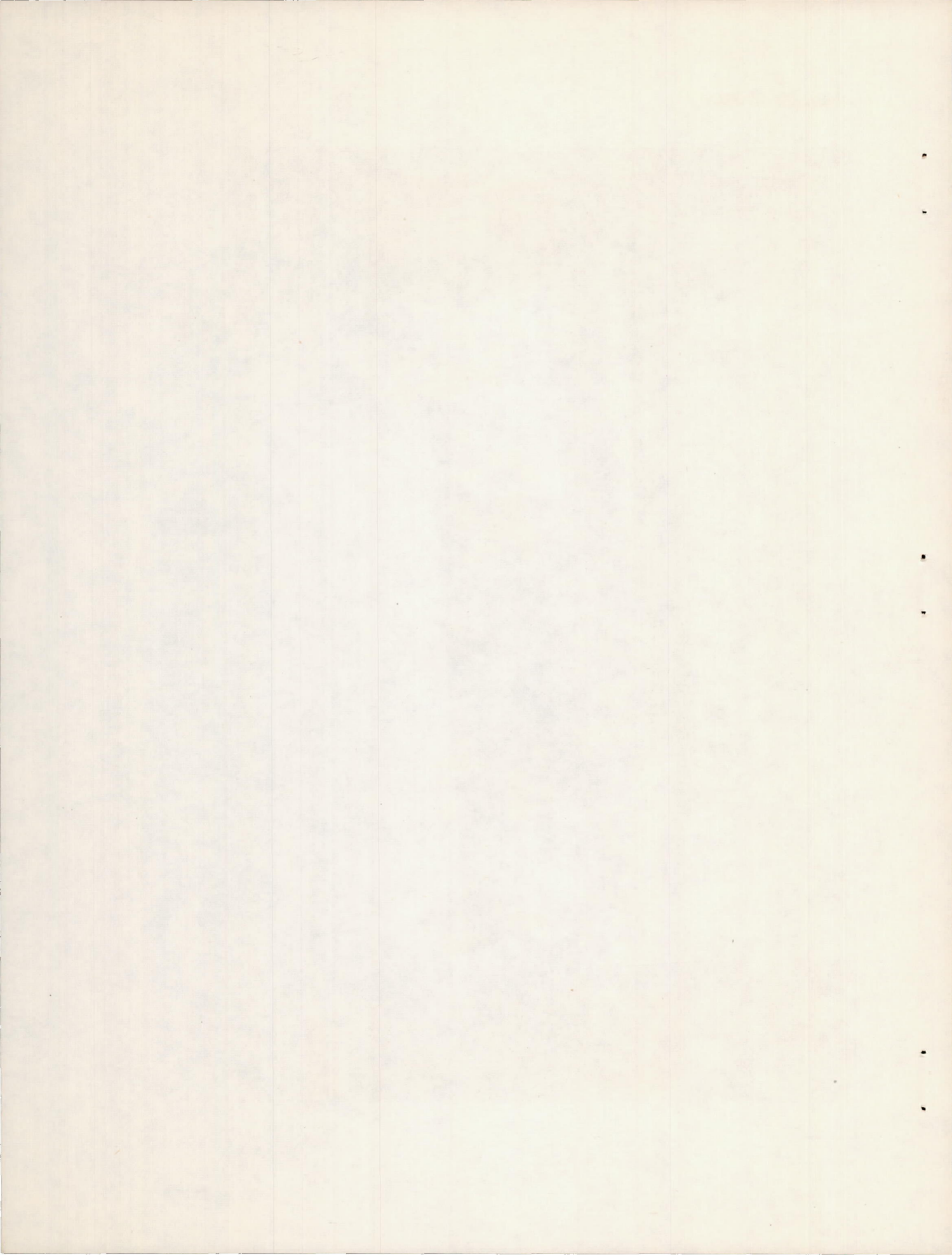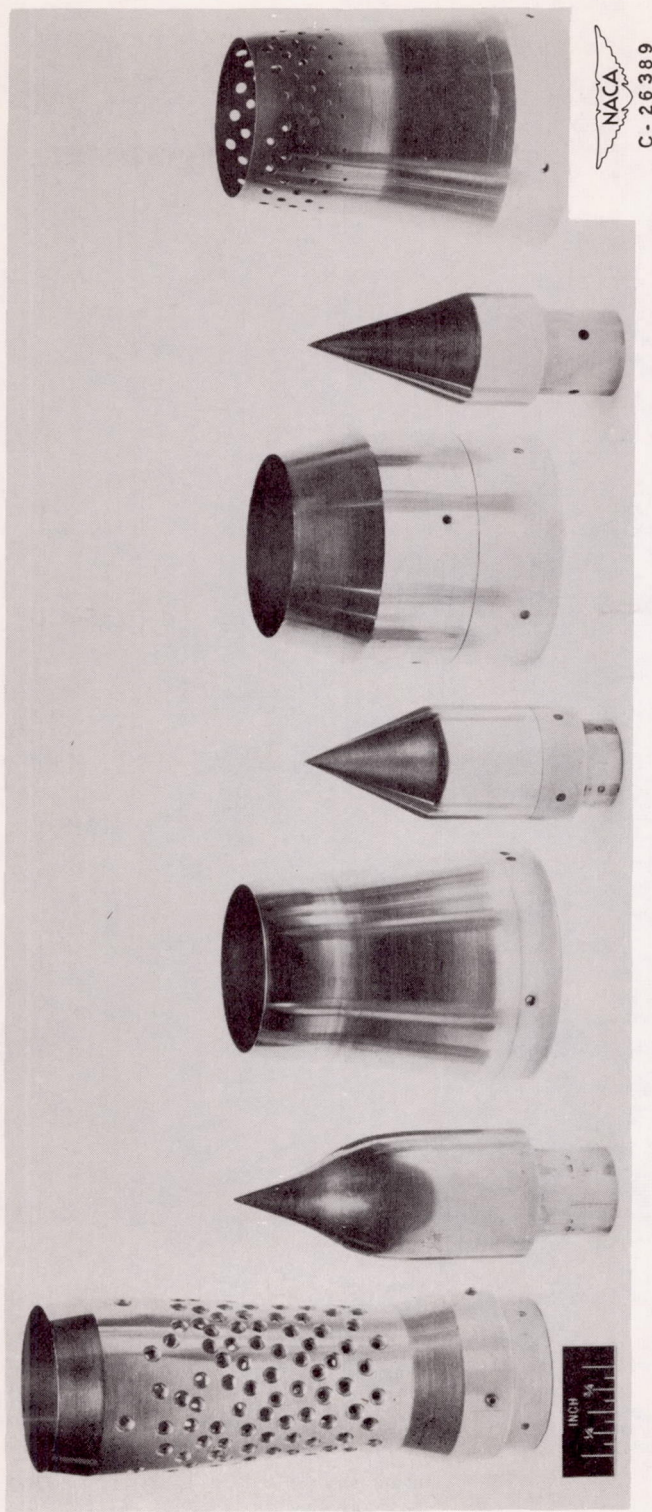
Figure 3. - Inlets and projecting spikes investigated.
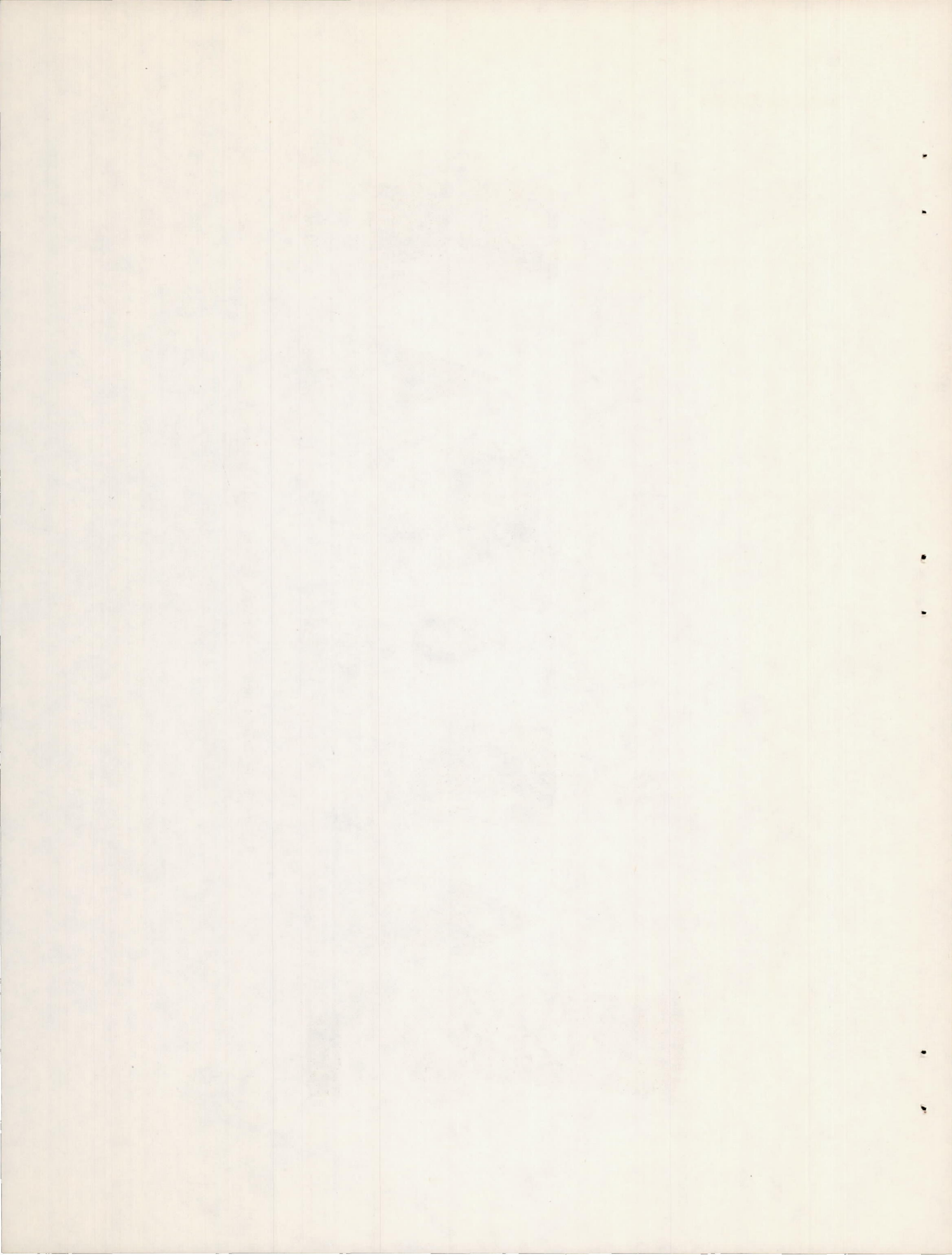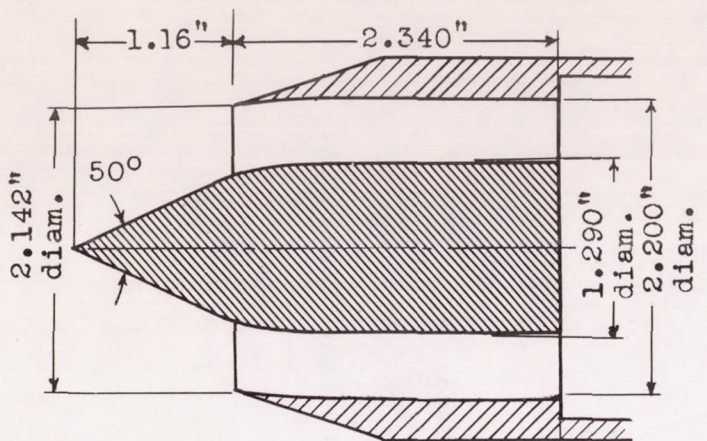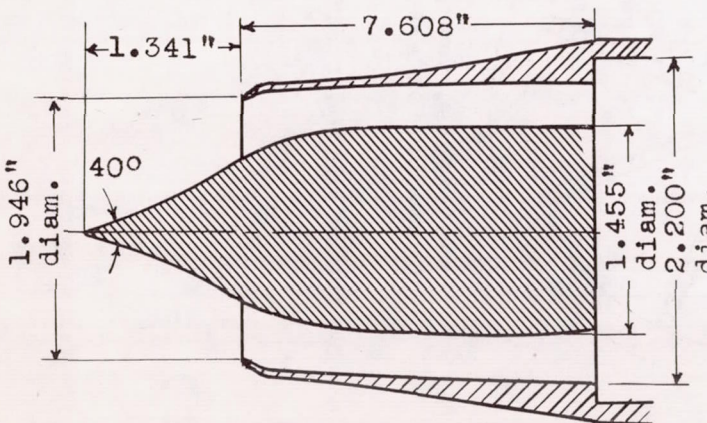
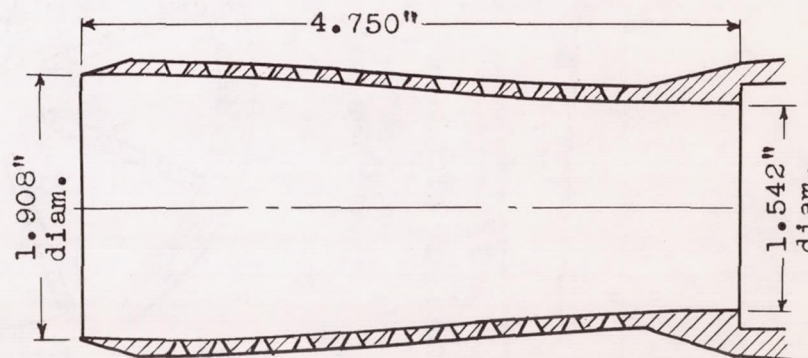Single-shock spike inlet
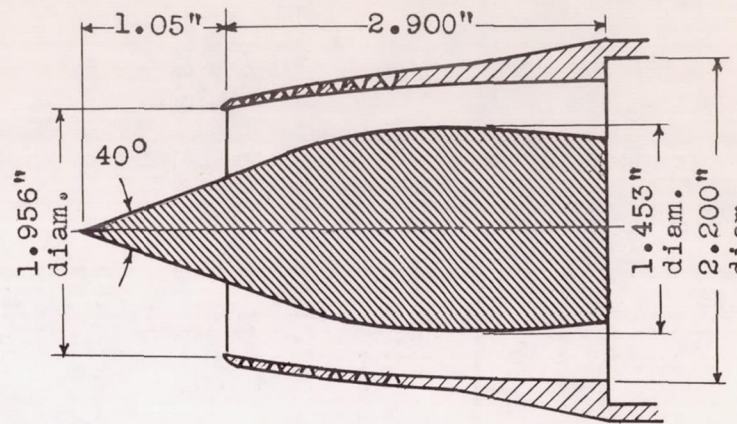
Single-shock spike with perforated cowl inlet

Curved-spike inlet

Perforated convergent-divergent inlet

Figure 4. - Inlet configurations investigated.

Conical
plug

Subsonic diffuser ——— Simulated combustion chamber

(a) Schematic diagram.

Diffuser	Length L (in.)	Diameter D (in.)
1	23.54	1.542
2	20.90	2.200

$R_2 = 0.99"$
$R_3 = 1.27"$
$R_4 = 1.51"$
$R_5 = 1.71"$
$R_1 = 0.57"$

(b) Pitot-static survey rake located
at station A-A.

NACA
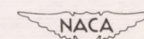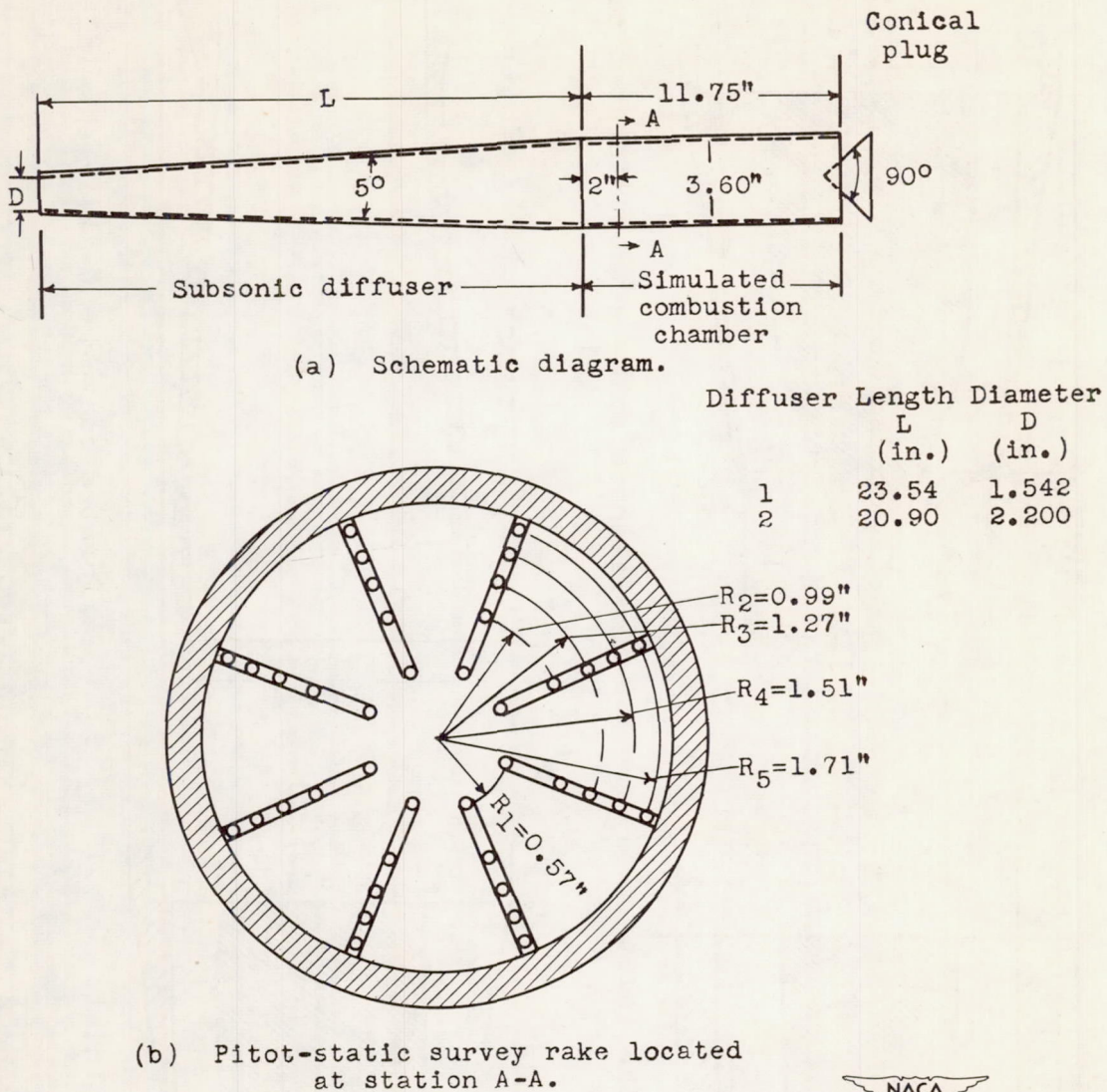
Figure 5. Sketch of subsonic diffuser and instrumentation.
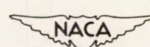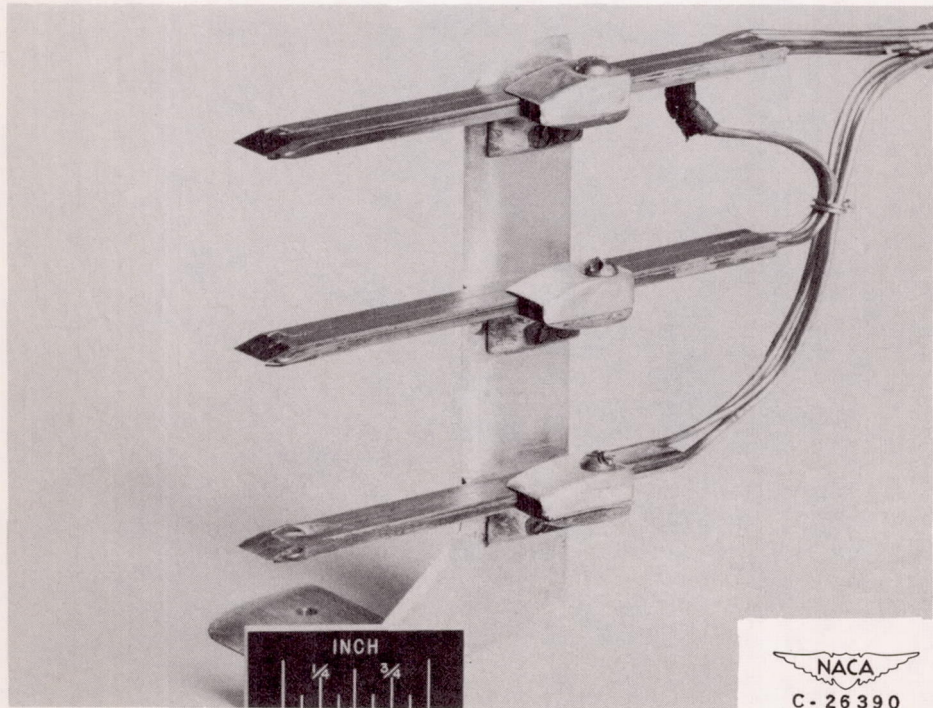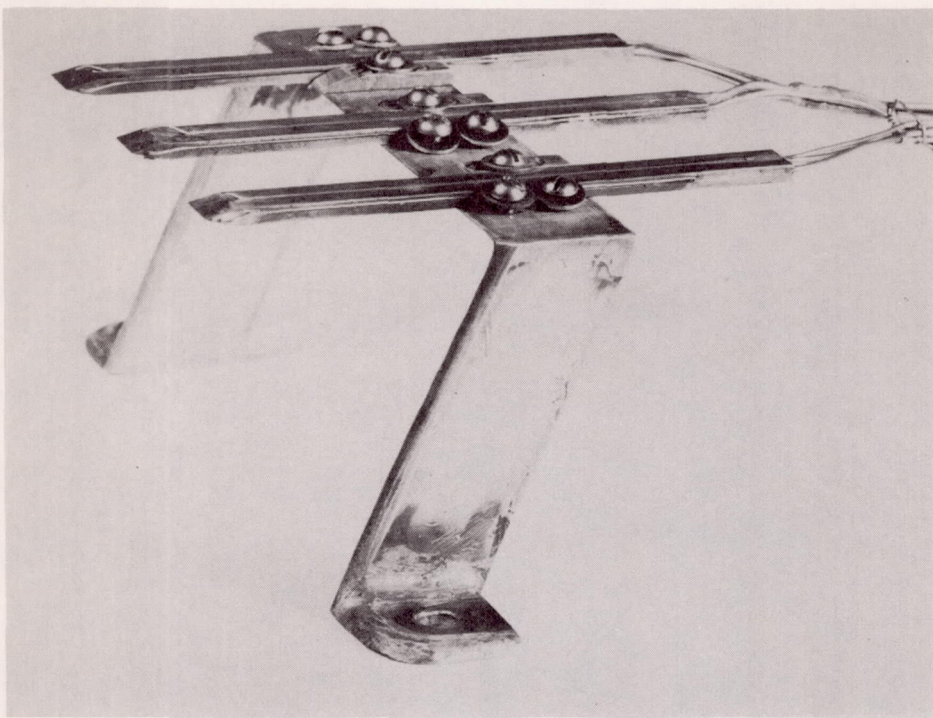
Figure 6. - Horizontal and vertical calibration wedge rakes.
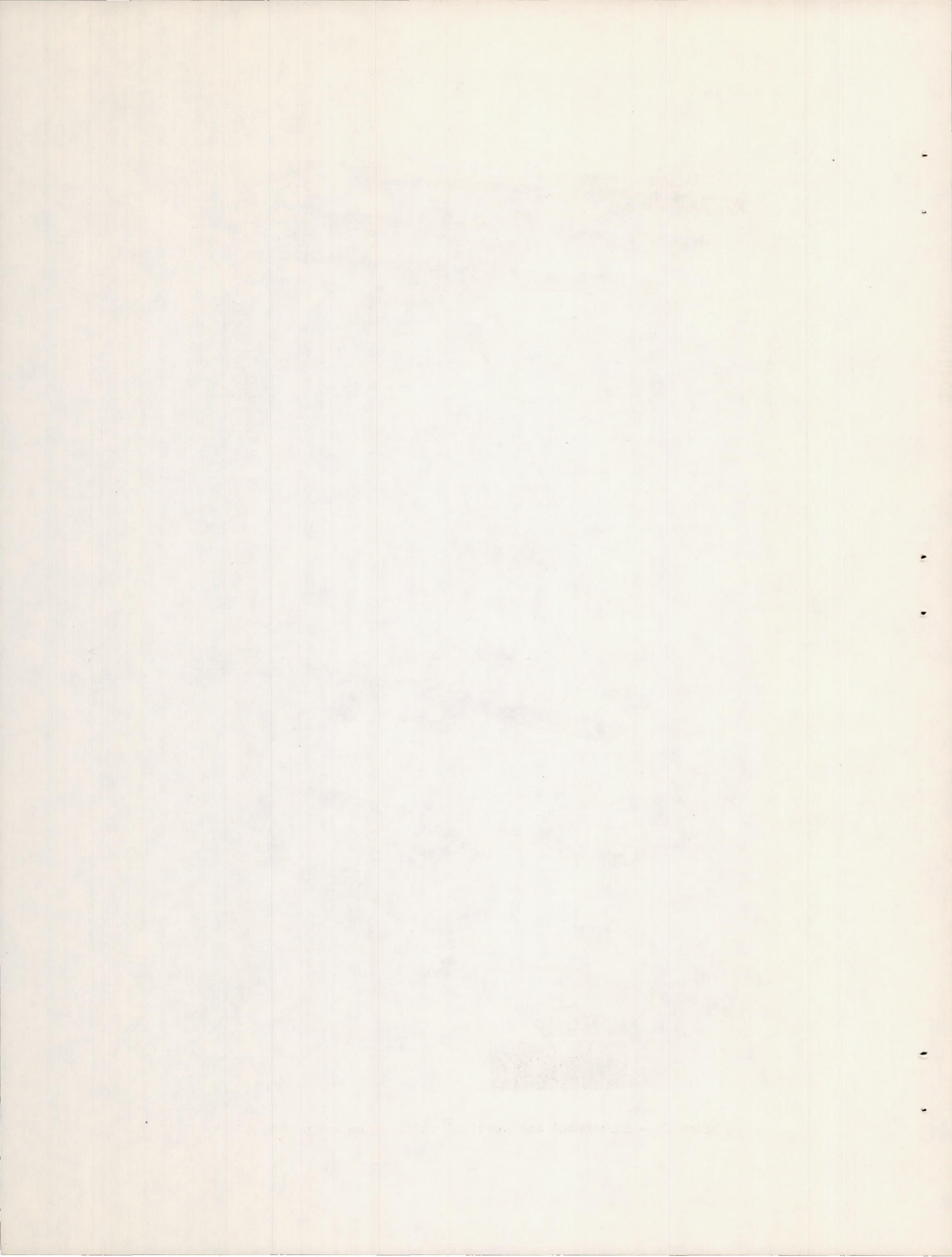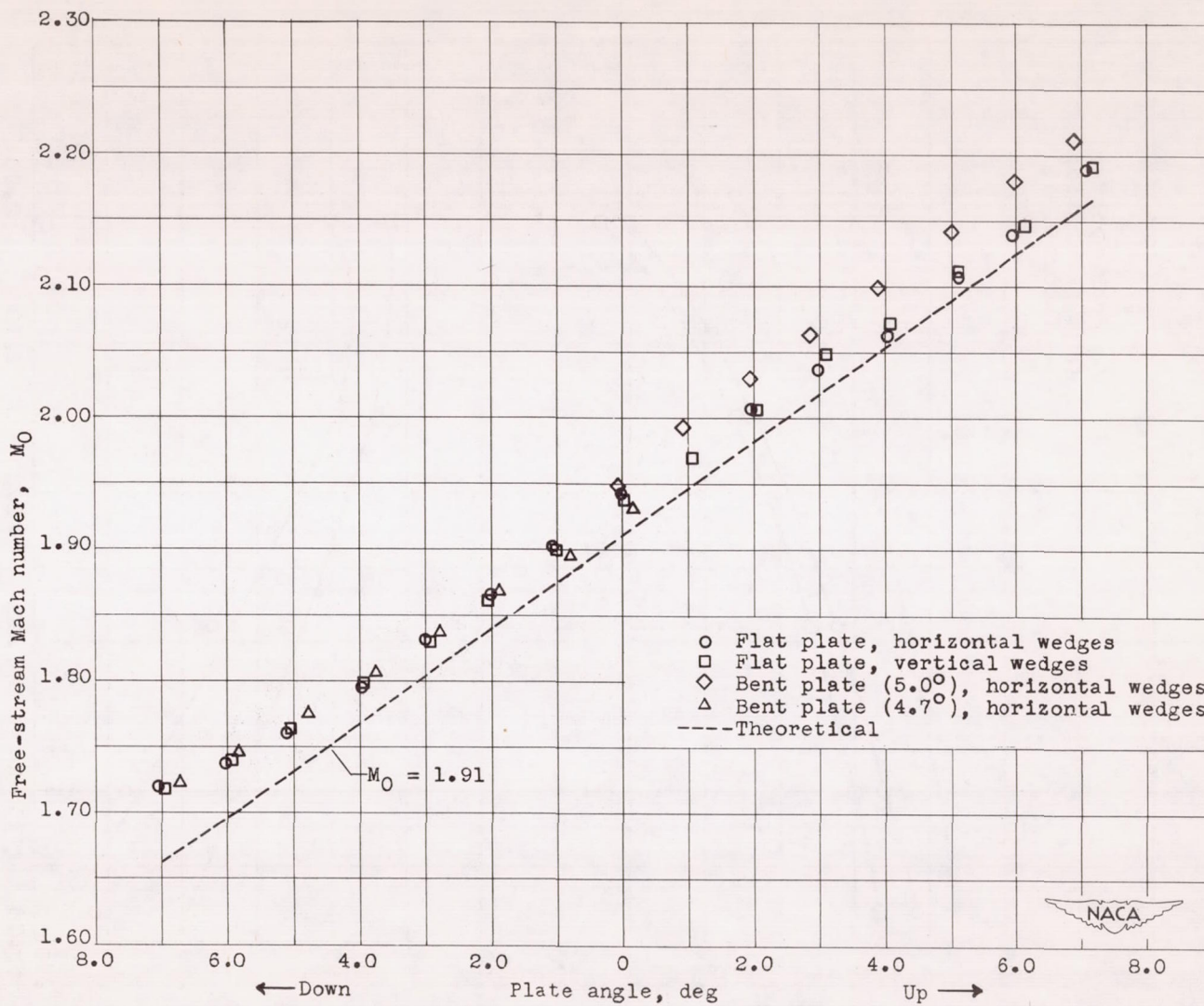
Figure 7. - Mach number calibration approximately 8 inches behind leading edge of plate as function of plate angle.
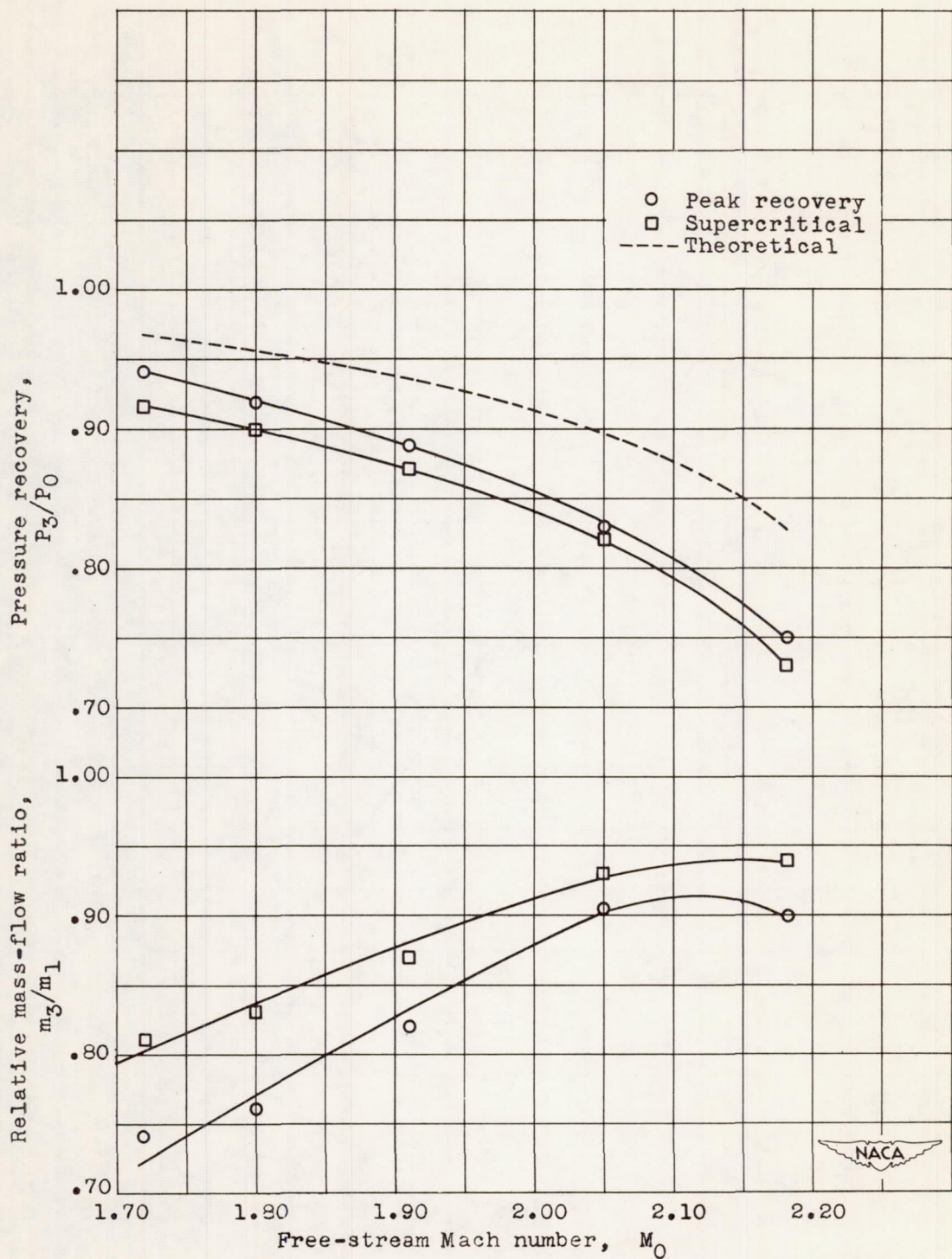
(a) Single-shock spike, curved cowl inlet.

Figure 8.- Pressure recovery and relative mass flow as function
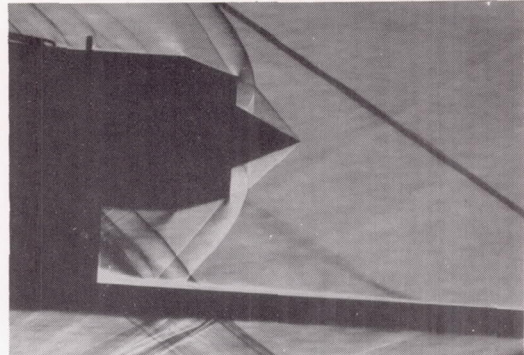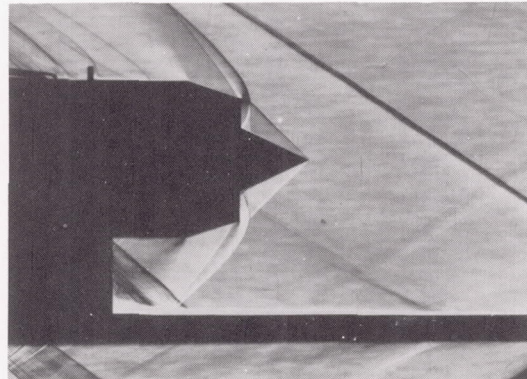of free-stream Mach number.
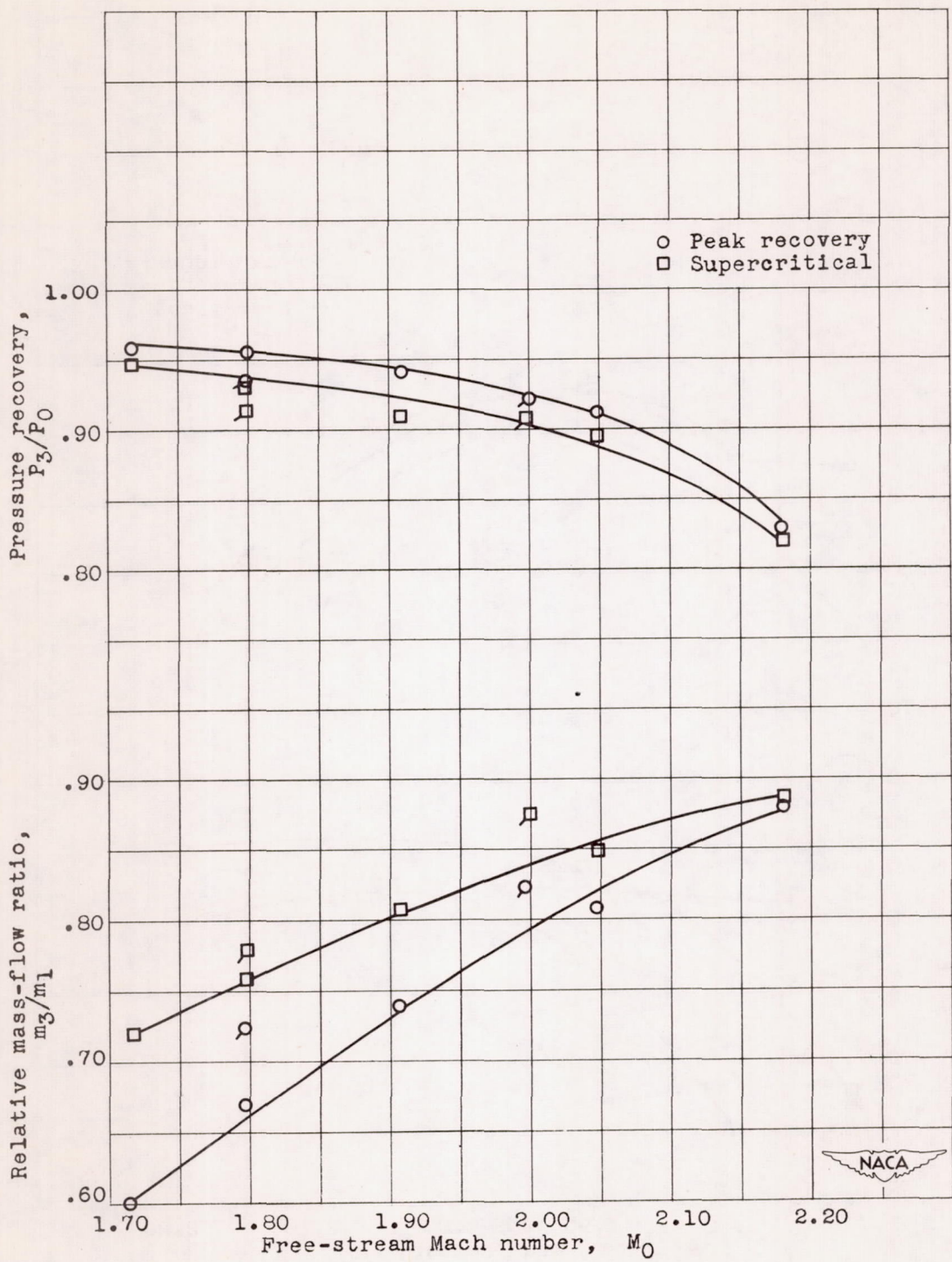
(b) Curved-spike inlet.

Figure 8. - Continued. Pressure recovery and relative mass flow
as function of free-stream Mach number.
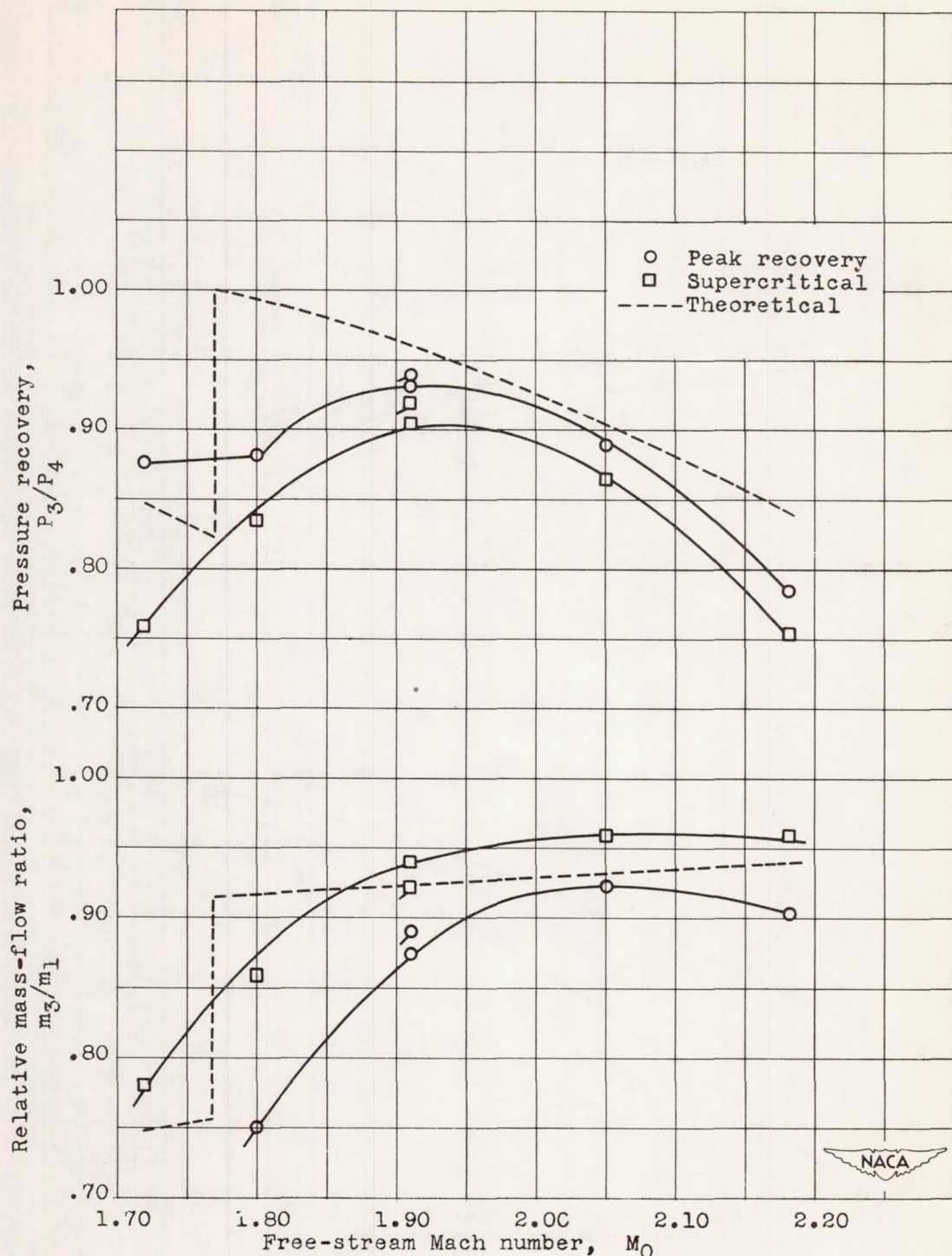
(c) Perforated convergent-divergent inlet.

Figure 8. - Continued. Pressure recovery and relative mass flow as
function of free-stream Mach number.
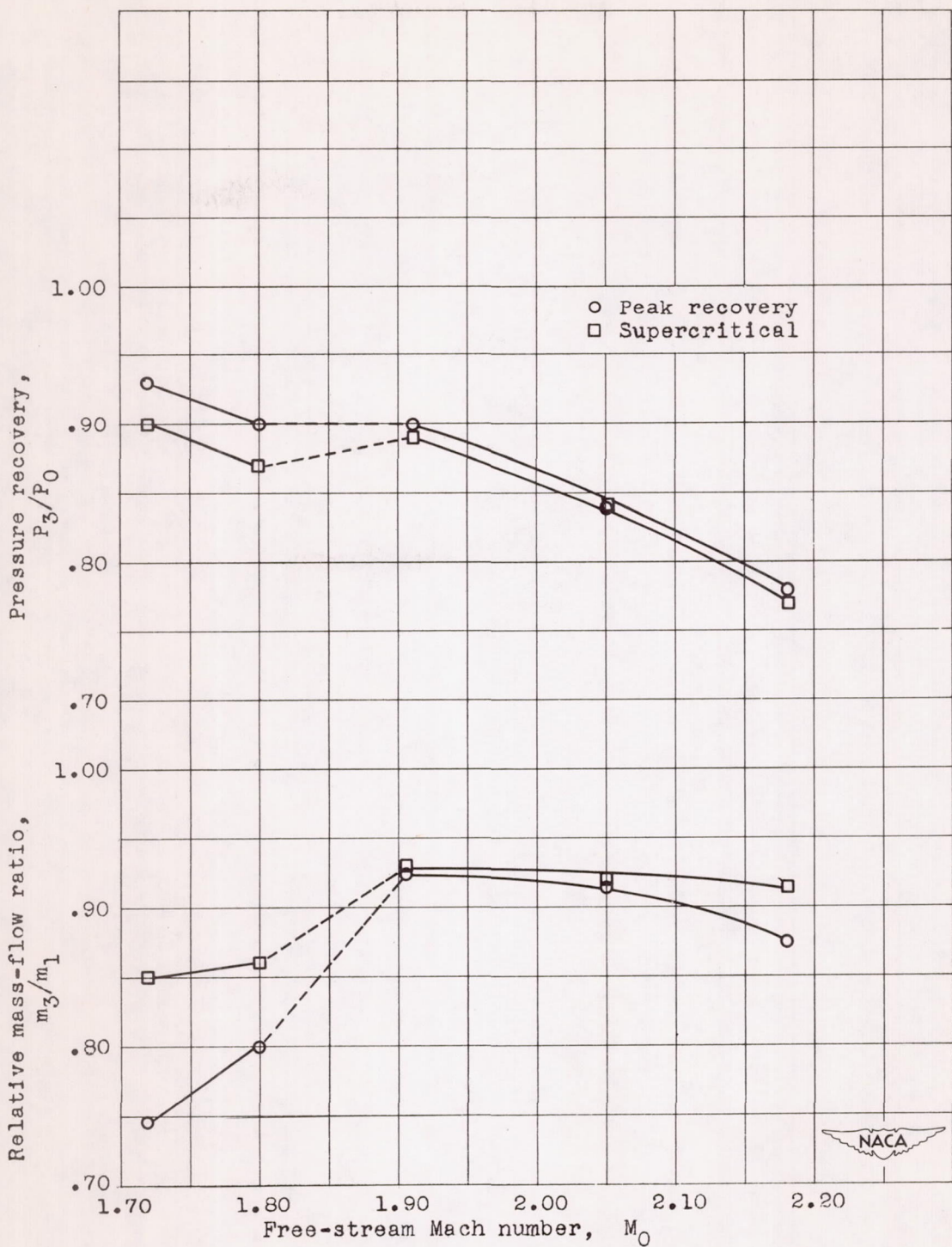
(d) Single-shock spike, perforated cowl inlet.

Figure 8. - Concluded. Pressure recovery and relative mass flow as
function of free-stream Mach number.
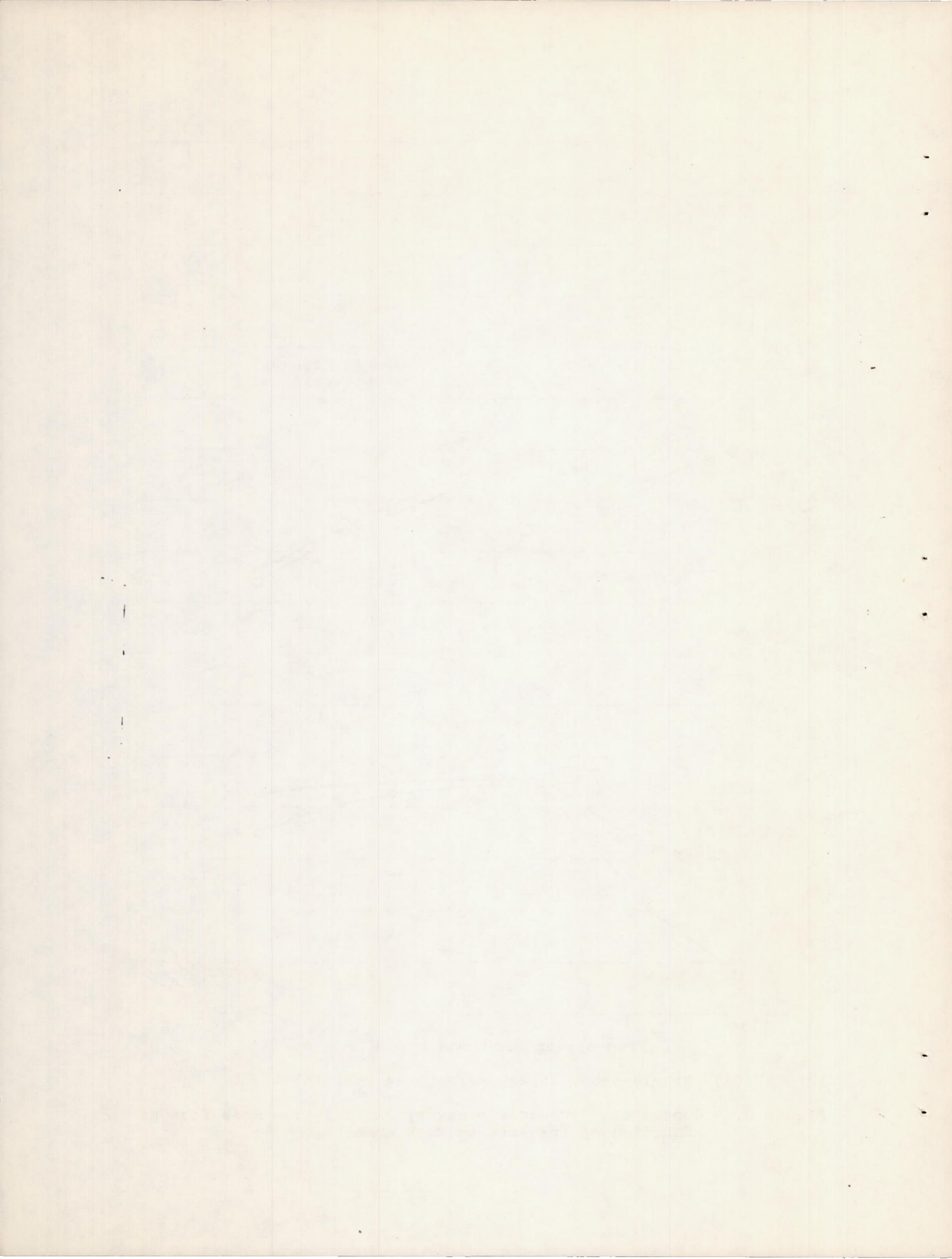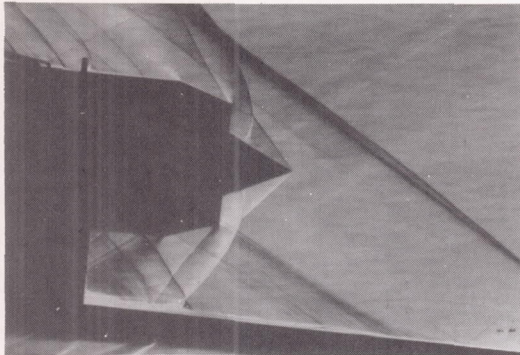
Free-stream Mach number M_0, 1.72;
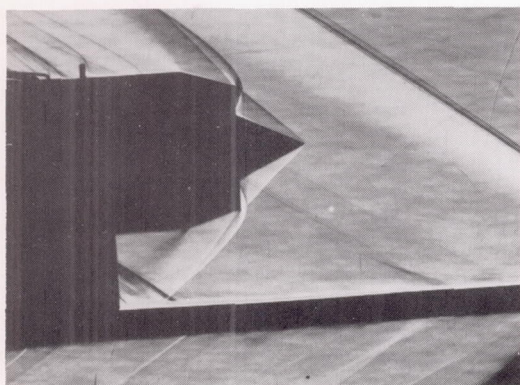P_3/P_0, 0.940; m_3/m_1, 0.740.

Free-stream Mach number M_0, 1.80;
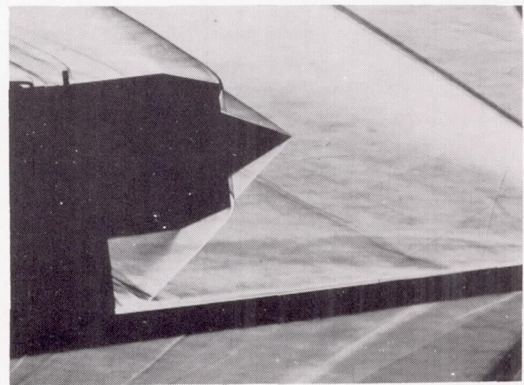P_3/P_0, 0.920; m_3/m_1, 0.760.

Free-stream Mach number M_0, 1.91;
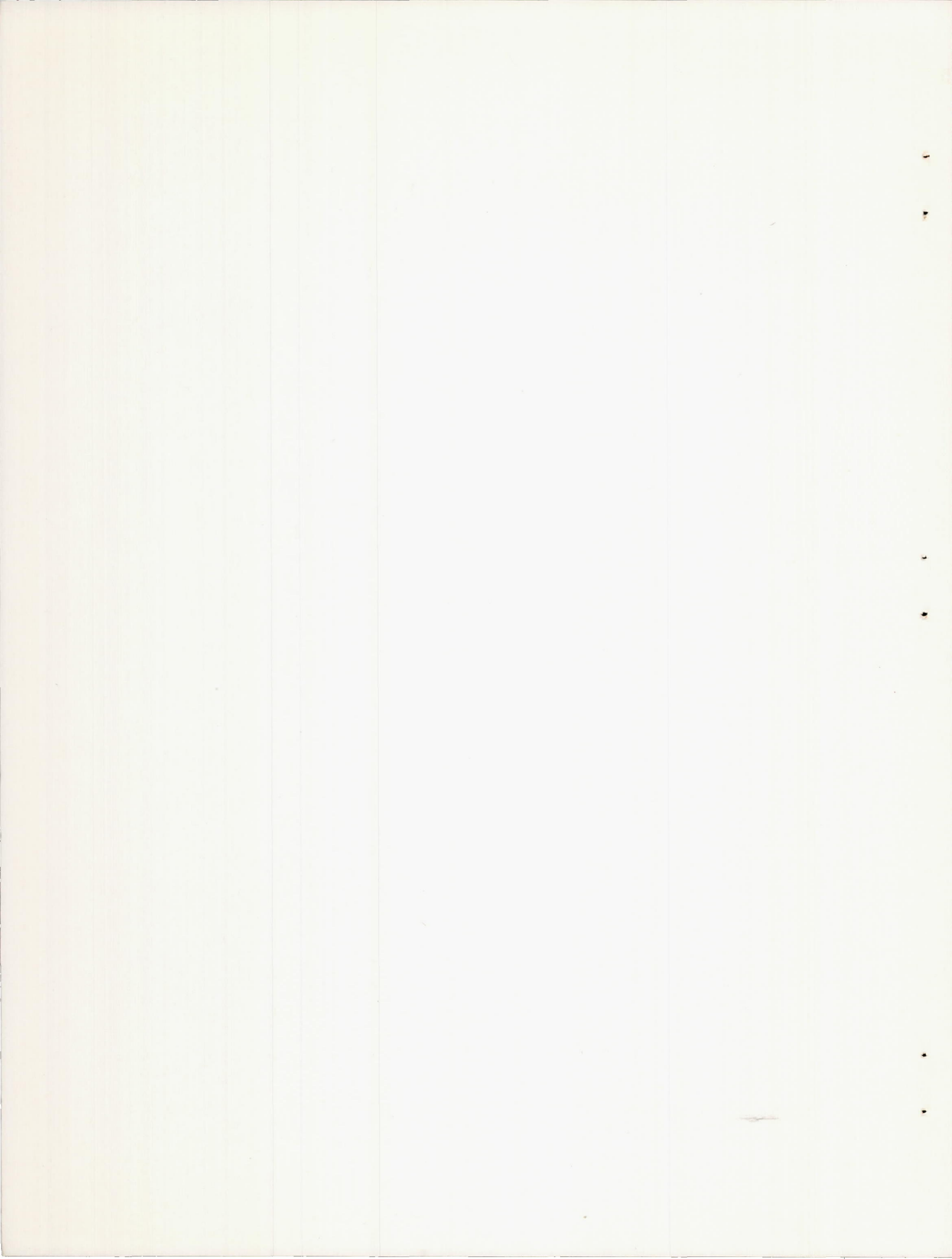P_3/P_0, 0.890; m_3/m_1, 0.820.

Free-stream Mach number M_0, 2.05;
P_3/P_0, 0.830; m_3/m_1, 0.905.

Free-stream Mach number M_0, 2.18.
P_3/P_0, 0.750; m_3/m_1, 0.900.

Figure 9. - Schlieren photographs of flow patterns in vicinity of single-
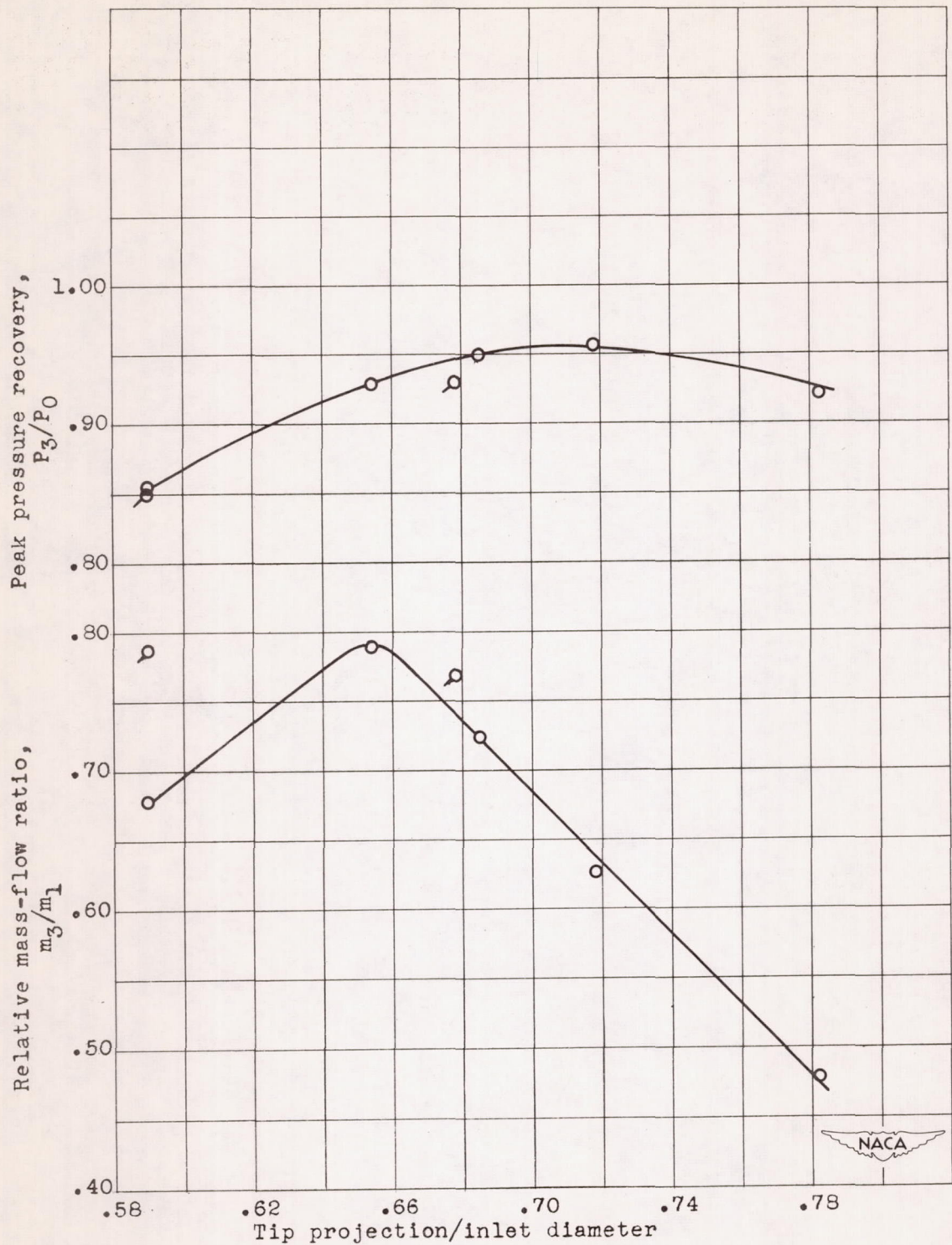shock spike inlet at point of peak recovery.

Figure 10. - Pressure recovery and mass-flow characteristics of curved spike inlet as function of dimensionless tip projection parameter. Free-stream Mach number M_0, 1.80.